

# Removal of Basic Blue-41 dye from Water by Stabilized Magnetic Iron Nanoparticles on Clinoptilolite Zeolite

SHIRIN AFSHIN<sup>1,2</sup>, YOUSEF RASHTBARI<sup>1,2</sup>, MEHDI VOSOUGHI<sup>1,3\*</sup>, RABIA REHMAN<sup>4\*</sup>,  
BAHMAN RAMAVANDI<sup>5</sup>, AYLAH BEHZAD<sup>1,2</sup>, LIVIU MITU<sup>6\*</sup>

<sup>1</sup>Students Research Committee, Faculty of Health, Ardabil University of Medical Sciences, Ardabil, Iran

<sup>2</sup>Department of Environmental Health Engineering, School of Public Health, Ardabil University of Medical Sciences, Ardabil, Iran

<sup>3</sup>Social Determinants of Health Research Center, Ardabil University of Medical Sciences, Ardabil, Iran

<sup>4</sup>Institute of Chemistry, University of the Punjab, Lahore-54590, Pakistan

<sup>5</sup>Department of Environmental Health Engineering, Faculty of Health and Nutrition, Bushehr University of Medical Sciences, Bushehr, Iran

<sup>6</sup>University of Pitesti, Department of Nature Sciences, 1 Targu din Vale Str., 110040, Pitesti, Romania

*In this work, Zeolite/Fe<sub>3</sub>O<sub>4</sub> nanocomposite used for adsorption of Blue 41 cationic dye from aqueous solutions in a wide range of concentrations. Analyses of FTIR, XRD, FESEM, VSM and XRF have confirmed the nature and the structure of Zeolite/Fe<sub>3</sub>O<sub>4</sub> nanocomposite adsorbent. The obtained results and analyzes determined that adsorption process efficiency increases by increasing reaction time, pH and amount of adsorbent and versus, increasing dye initial concentration causes significant decrease of adsorption efficiency. The obtained results of adsorption of isotherm and kinetics study illustrated that data follows Freundlich model and pseudo second order kinetics. Under optimum conditions of pH = 9, dye initial concentration of 100 mg/L, adsorbent dose of 3 g/L and reaction time of 60 min, removal efficiency was obtained 71.4 %. Totally results showed that Zeolite/Fe<sub>3</sub>O<sub>4</sub> nanocomposite can be used by scrutiny of operating conditions of the adsorption process as a adsorbent with high effectiveness and availability, eco-friendly and cost-effective in order to removing dye from waste water of different industries.*

**Keywords:** Zeolite/Fe<sub>3</sub>O<sub>4</sub> nanocomposite, Blue 41 cationic dye, Adsorption, Cleaner production

Now a days, with the development of cities and various industries, the importance of controlling environmental pollution has been increased. Therefore, the treatment and disposal of waste water polluted to dye is one of the most serious environmental problems [1]. Colours are widely produced in various industries such as food, leather, paper, polishing oils, pharmaceuticals, cosmetics industries and etc. [2]. One of the most important dye consumer industries is the textile industry, which produces strong dye sewage at a concentration of 10 to 200 mg/L [3]. Estimates indicate that around 700,000 tons of dyes are produced world wide every year, which about 15 percent are introduced into the environment without any treatment process [4]. Dyes are aromatic organic compounds that absorb the light in the wave length of 350-300 nm (visible light) and are considered as one of the fundamental environmental problems [5]. Most of the dyes used in the industry have carcinogenesis and mutagenesis properties and can cause allergies, dermatitis, skin irritation and cancer in humans [6].

The cationic dyes have azo structure, in which one or more bonds (N = N) are attached to the aromatic rings. The aromatic rings of dye have caused resistance to degradation by conventional waste water treatment processes and on the other hand, cationic dyes are more toxic than anionic dyes [7].

Different methods have been proposed and used for the treatment of dyes sewage. Among the available techniques to remove the dye can be pointed to biological treatment methods [8], sonochemical [9], photo-fenton [10], photocatalysis [11], natural adsorbents [12] and adsorption [13]. The use of biological methods has been difficult due to the low ratio of COD/BOD<sub>5</sub> about 0.25, the high toxicity of dyes for available microorganisms in the process, having tolerant and complex structures of dyes compounds and on the other hand, the use of this method requires a long time and controlled conditions. Some of the above methods by producing high amounts of sludge, being uneconomical and operation problems have limited the use of them in many countries [14]. Among the above-mentioned methods, adsorption surface due to easy operation, low investment costs, insensitivity to toxic substances, the ability of dyes concentrated waste water treatment and the possibility of reuse of adsorbent through reduction is considered as an effective technique for decolourisation of sewage [15]. One of the most useful adsorbent is the adsorption of activated carbon process. One of the serious problems in the utilization of activated carbon is the high cost of production and its reduction. Therefore, in recent years, many studies have carried out to find cheaper and more effective adsorbents [16]. The most extended and useful natural adsorbents have been clinoptilolite zeolite, which have the high capacity of ion exchange and have many internal and external surfaces. The other important feature of this zeolite is possibility of its reduction by maintaining initial properties [3]. Zeolite is a family of hydrated

\*email:mvn\_20@yahoo.com; grinorganic@yahoo.com; ktm7ro@yahoo.com

alumina silicates of alkaline and earthy alkaline metals with crystalline and tetrahedral structure (four atomic oxygen in around one atomic silicon). There are holes and channels of 3-10 Å inside them. Three important properties of ionic exchange, adsorption and catalyticity have been due to the structural properties of zeolites, which have led to many applications in various branches of the industry, especially in environmental processes [17, 18]. However, due to the very small dimensions of these adsorbents, the possibility of separation after doing process has always faced with difficulty and so there are various methods for stabilization or separation of aqueous solutions. One of these methods of separating the adsorbents is magnetizing with magnetic particles which after doing the adsorption process, the adsorbent has separated from solution by creation of a magnetic field and is reduced [19]. The presence of iron oxide nanoparticles ( $\text{Fe}_3\text{O}_4$ ) in the adsorbent structure leads to chemical stability and excellent recycling ability of adsorbents. However, magnetic separation techniques have been recently investigated in different studies widely due to low-cost, simplicity and high speed of separation and also high efficiency [20]. Since various studies have not reported any performance of magnetic zeolite for removing Blue 41 cationic dye, investigating its efficiency in removal of Blue 41 cationic dye affected by various variables on the process, including pH, reaction time, adsorbent dose and initial dye concentration in synthetic solutions were studied. Finally, the kinetics of the reaction and the adsorption isotherm were determined to removal of dye.

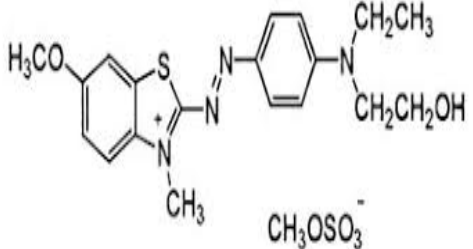
## Experimental part

### Materials and methods

#### Chemical materials required

Blue 41 cationic dye used in this research was made by Alvan Sabet Hamedan. The general specification of dye is presented in (table 1) [13].  $\text{H}_2\text{SO}_4$  and NaOH 0.1 M were used to set out the pH of the solution containing dye. All substances used in experiments were prepared from Germany, Merck Company, with laboratorial degree of purity. It should be noted that at all stages of experiments, double distilled water was used.

**Table 1**  
SPECIFICATIONS OF BLUE 41 DYE

Chemical structure	Chemical formula	Molecular weight
	$\text{C}_{20}\text{H}_{26}\text{N}_4\text{O}_6\text{S}_2$	482.573 g/mol

#### Analysis tools

The residual concentration of Blue 41 dyes was measured by the HACH DR-5000 spectrophotometer, Canada. Its wave length was 617 nm [21]. FTIR analysis was performed to determine the available functional groups on adsorbent level by Perkin Elmer device of the Spectrum two model in range of 450-14000 cm. X-ray diffraction for Nanocomposite was determined in the range of  $2\theta = 80-10^\circ$  by XRD device (Philips PNA-analytical diffractometer, Netherlands). For determining the surface and morphological characteristics of adsorbent, FESEM scanning electron microscope at accelerative voltage of 10 kV was used. Magnetic properties measurement (VSM) were used to investigate magnetic properties, magnetic phases and residue loop, which is a kind of visual expression of material magnetism. The gas adsorption analysis based on the measurement of the volume of adsorbed and desorbed nitrogen gas by the level of substance at a constant temperature of liquid nitrogen (77°K) to calculate the volume of pores and area of surface by the BET device (Quantachrome Instruments, CHEMBET 3000 model, China). Chemical compounds of adsorbent were performed by using X-ray spectroscopy (XRF) (Philips-Magix Pro., Philips Electronics Co., Netherlands).

#### Preparation of Clinoptilolite Zeolite

After preparation of clinoptilolite zeolite, granulation was performed by using ASTM standard sieves. Then, to isolate impurities in clinoptilolite zeolite, was washed several times with distilled water by using a Whatman filter. Finally, the adsorbent was dried in the oven for 24 hours at 250°C [22].

### *Synthetic of Fe<sub>3</sub>O<sub>4</sub> nanoparticles*

Fe<sub>3</sub>O<sub>4</sub> magnetic nanoparticles were synthesized by chemical coprecipitation method. In this method, first, in a rounded balloon, in atmosphere of nitrogen gas, amount of 5.4 g FeCl<sub>3</sub>·6H<sub>2</sub>O and 2.78 g FeCl<sub>2</sub>·4H<sub>2</sub>O (in weight ratio of two to one) was mixed in 100 mL of ion-free water. 25 % of aqua ammonia was added to solution on shaker drop by drop until the pH of solution become 9 and at last, black scale, which has magnetic nanoparticles, was formed. The formed Fe<sub>3</sub>O<sub>4</sub> magnetic nanoparticles were mixed by magnetic stirrer for 30 minutes. Then, it was heated in 75°C, at last stage, the formed Fe<sub>3</sub>O<sub>4</sub> magnetic nanoparticles were washed three times by distilled water and then washed twice by ethanol [23].

### *Loading Clinoptilolite Zeolite on Fe<sub>3</sub>O<sub>4</sub> magnetic nanoparticles*

For loading Fe<sub>3</sub>O<sub>4</sub> magnetic nanoparticles on clinoptilolite zeolite, submergence was utilized. After preparation of clinoptilolite zeolite and synthesis of Fe<sub>3</sub>O<sub>4</sub> nanoparticles, 7.5 g of zeolite (in weight ratio of 100 to 25) was added to 200 mL of distilled water and mixed by magnetic stirrer for 60 minutes. 2.5 g of Fe<sub>3</sub>O<sub>4</sub> nanoparticles were added to the solution containing zeolite and homogenization was done in ultrasonic device for 60 minutes at temperature of 70°C. The solution was on the magnetic stirrer at the rate of 300 rpm until the loading process of magnetic nanoparticles on zeolite to be done. The resultant zeolite/Fe<sub>3</sub>O<sub>4</sub> nanocomposite was washed several times by distilled water and then was separated by the magnet of 1/3 T and finally was dried for 12 hours at temperature of 70°C [24].

### *Determining pH of the zero point*

To survey the adsorbent superficial load, pH analysis of the zero point ( $pH_{pzc}$ ) was investigated. To determine  $pH_{pzc}$ , NaCl solution of 0.01 M as electrolyte and sulfuric acid solutions and caustic soda as pH controller factors were utilized. At first, the pH of solutions were adjusted in (2,3,4,5,6,7,8,9,10,11 and 12) and then, the amount of 0.01 g/L of adsorbents was added to Erlens of 100 mL and was mixed at rates of 150 rpm for 48 hours. After the mentioned time, pH was read.  $pH_{pzc}$  point from plotting the initial pH values against the final pH values was determined. The point of intersection of the lines with a smooth line is the point of zero adsorbents [25].

### *Adsorption experiments*

The stock solution of Blue 41 cationic dye was prepared by dissolving the powder of Blue 41 cationic dye in double distilled water with concentration of 1000 mg/L. Adsorption experiments were carried out by dyes solutions with change of pH (3-5-7-9-11), amount of adsorbent (0.25-0.5-1-1.5-2 g/L), concentration of dye (50-100-150 mg/L), contact time (5-10-15-30-45-60-75 min). After ending determined reaction time, solution was centrifuged by centrifuge device at rate of 3000 rpm for 5 minutes and amount of adsorption of dye was read by using spectrophotometer device. Finally, after adsorption process, removal efficiency, amount of dye adsorption per mass unit for Blue 41 cationic dye were respectively determined by equations (1) and (2) [26, 27].

$$\text{Removal efficiency (\%)} = \frac{C_0 - C_t}{C_0} \times 100 \quad (1)$$

$$\text{Adsorption capacity (mg/g)} = \frac{(C_0 - C_t) \times V}{M} \quad (2)$$

Which in them,  $C_0$  and  $C_t$  are respectively initial and final concentration of dye in solution based on mg/L, volume of solution (V) based on liters and adsorbent mass (M) based on g.

## **Results and discussions**

### *Investigating structural nature of the adsorbent*

FTIR analyses provide the structural and combinations information about functional groups of samples. FTIR analysis of zeolite and zeolite/Fe<sub>3</sub>O<sub>4</sub> nanocomposite was observed in (Figure 1). The resultant spectrum of FTIR was used before adsorption process of Blue 41 cationic dye to determine vibratory frequency changes in functional groups. According to the chart, it is defined that in the position of most of the bands hasn't been any change which indicates preserving crystalline structure of zeolite after becoming magnetized; in position of 3400-3600 cm<sup>-1</sup> in zeolite and composite is related to stretching vibrations of O—H of free hydroxyl, and the position of 3200-3500 cm<sup>-1</sup> with peak at 3436 cm<sup>-1</sup> in zeolite and composite is related to stretching vibrations of O—H bond in water molecule [28]. The observed peak at bond of 1055 cm<sup>-1</sup> is related to vibration of Al—O—Si and the observed peaks at 467 cm<sup>-1</sup>, 548 cm<sup>-1</sup>, 793 cm<sup>-1</sup> is respectively related to expansion structure of Si—O—Si [29]. In addition, maximum adsorption of peak at 1401 cm<sup>-1</sup> is illustrator of Fe—O structure in Fe<sub>3</sub>O<sub>4</sub> which confirms the successful coating of Fe<sub>3</sub>O<sub>4</sub> in surface of zeolite [30].

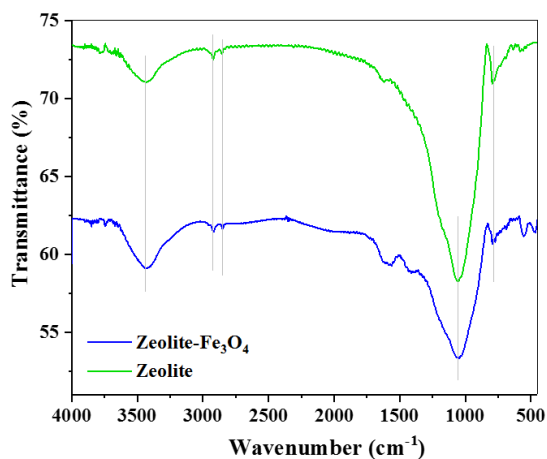


Fig. 1. FT-IR spectrum of zeolite and zeolite/Fe<sub>3</sub>O<sub>4</sub> nanocomposite

#### Adsorbent specific level analysis using nitrogen adsorption

Gas adsorption analysis based on the measurement of absorbed and desorbed nitrogen gas by the substance surface at the constant temperature of liquid nitrogen (77°K) to calculate the volume of pores and area of surface. This analysis has been accomplished by BET device. The absorbed and desorbed isotherms of N<sub>2</sub> were conducted for zeolite and nanocomposite. The adsorption isotherm has followed type IV. By comparing (Fig. 2) can be found that the porosity of the nanocomposite is more than zeolite. The area of specific surface of zeolite and nanocomposite is respectively calculated 147.52 m<sup>2</sup>/g and 163.98 m<sup>2</sup>/g (table 2). Also, the total volume pores in zeolite and nanocomposite has respectively been 0.3249 cm<sup>3</sup>/g and 0.3587 cm<sup>3</sup>/g and is indicator the amount of volume of pores in composite. The result shows that by adding Fe<sub>3</sub>O<sub>4</sub> nanoparticles to zeolite, the area of adsorbent surface has increased. The maximum pores of adsorbents were in range of 1-4 nm which is illustrator of microscopic structure.

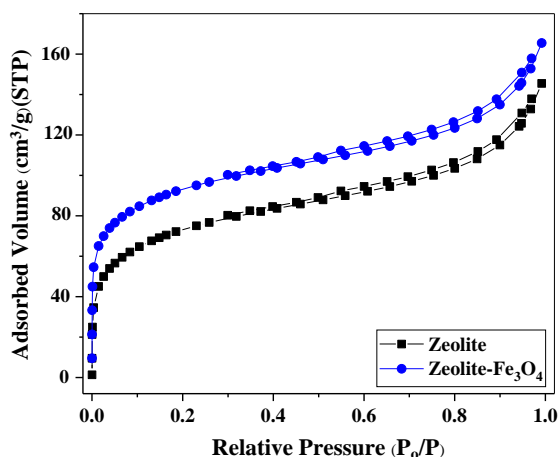


Fig. 2. Adsorption-desorption isotherms for zeolite and nanocomposite

**Table 2**  
THE AREA OF SPECIFIC SURFACE AND TOTAL VOLUME OF PORES  
USING GAS ADSORPTION ANALYSIS

Material	S <sub>BET</sub> (m <sup>2</sup> /g)	S <sub>micro</sub> (m <sup>2</sup> /g)	S <sub>meso</sub> (m <sup>2</sup> /g)	V <sub>Total</sub> (cm <sup>3</sup> /g)	V <sub>micro</sub> (cm <sup>3</sup> /g)	V <sub>meso</sub> (cm <sup>3</sup> /g)
zeolite	147.52	65.14	82.4	0.3249	0.1112	0.2137
Zeolite-Fe <sub>3</sub> O <sub>4</sub>	163.98	71.45	92.53	0.3587	0.1984	0.1603

#### Investigation of elemental decomposition of bentonite adsorbent using XRF analysis

The result of XRD analysis (table 3) confirms the presence of silica and alumina as the main components with trace amount of sodium, magnesium, potassium, iron and titanium dioxide as impurity in clinoptilolite zeolite compound. Zeolite analysis, which is mostly containing silicon and aluminum with Si/Al ratio of 4/1, indicated that according to conducted studies, in natural zeolites with Si/Al ratio more than 4, zeolite is clinoptilolite type [31]. The amount of CaO as well as Na<sub>2</sub>O is representative of the presence of calcite and sodium among the clinoptilolite layers. On the other hand, the results show that most of the aluminums are in form of clinoptilolite so it is expected that absorbed contaminant types are mainly removed by SiO<sub>2</sub> or Al<sub>2</sub>O<sub>3</sub> [32].

**Table 3**  
ELEMENTAL ANALYSIS OF NATURAL ADSORBENT OF CLINOPTILOLITE

Sample	SiO <sub>2</sub>	Al <sub>2</sub> O <sub>3</sub>	Fe <sub>2</sub> O <sub>3</sub>	CaO	Na <sub>2</sub> O	MgO	K <sub>2</sub> O	TiO <sub>2</sub>	MnO	P <sub>2</sub> O <sub>5</sub>	LOI
<b>Zeolite</b>	42.081 %	10.247 %	6.119 %	12.351 %	0.381 %	5.182 %	2.661 %	0.557 %	0.138 %	0.128 %	20.1 %

#### *Surveying the structure and nature of adsorbent using XRD analysis*

For determining the crystalline phase of nanocomposite and doing measurement of their structural characteristics, XRD pattern has been shown in the angle of about  $2\theta$  in (Figure 3). XRD registered pattern for zeolite clinoptilolite shows that in the structure of zeolite clinoptilolite, in addition to Montmorillonite as clay mineral which contains the most and the main part of zeolite clinoptilolite, there are amount of non-clay impurities too, including Quartz, Calcite and Feldspar. The formation of sharp and stretched peaks especially in the  $2\theta$  region are  $24.5^\circ$  and  $27^\circ$ , which are respectively related to clinoptilolite and quartz, it is proving on the high crystallinity of the adsorbent [31]. The formed peaks at angles of  $30.6^\circ$ ,  $35.88^\circ$ ,  $43.53^\circ$ ,  $53.4^\circ$ ,  $57.1^\circ$  and  $62.6^\circ$  in the X-ray diffraction pattern of Fe<sub>3</sub>O<sub>4</sub> nanoparticles illustrate the presence of iron oxide particles in the Fe<sub>3</sub>O<sub>4</sub> nanoparticles structure and therefore this analysis show that iron particles have been synthesized successfully and have been galvanized on zeolite [33].

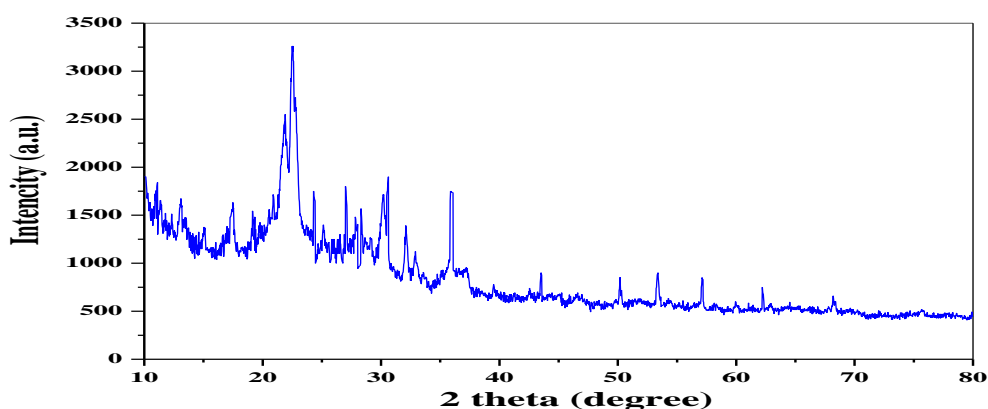


Fig. 3. XRD of zeolite/Fe<sub>3</sub>O<sub>4</sub> nanocomposites

#### *Morphological survey of the adsorbent using FESEM analysis*

FESEM analysis has been indicated morphological surface of zeolite, Fe<sub>3</sub>O<sub>4</sub> nanoparticles and zeolite/Fe<sub>3</sub>O<sub>4</sub> nanocomposite before adsorption of Blue 41 cationic dye in (Figure 4). As it is seen in (Figure 4-a), zeolite Clinoptilolite has a laminar and compact structure. In some cases, unsteady changes are seen that can be related to probable diminution of areas of some clay particles [34]. According to the (Figure 4) steady appearance with bumps and small swellings (Figure 4-b) is illustrator of Fe<sub>3</sub>O<sub>4</sub> nanoparticles that it has a regular morphology and they have put together steady, homogenous, spherical. Particles' size were determined about 30 nm [35]. From (Figure 4-c) was observed that some of Fe<sub>3</sub>O<sub>4</sub> nanoparticles tend to combine with zeolite. The accumulation of cluster shape is evident among them. The white particles, which have been shown on the zeolite in (Fig. 4-c), are illustrator of presence of Fe<sub>3</sub>O<sub>4</sub> on the surface of this nanocomposite. The rough and rugged levels of Fe<sub>3</sub>O<sub>4</sub> nanoparticles increase the adsorption sites of zeolite.

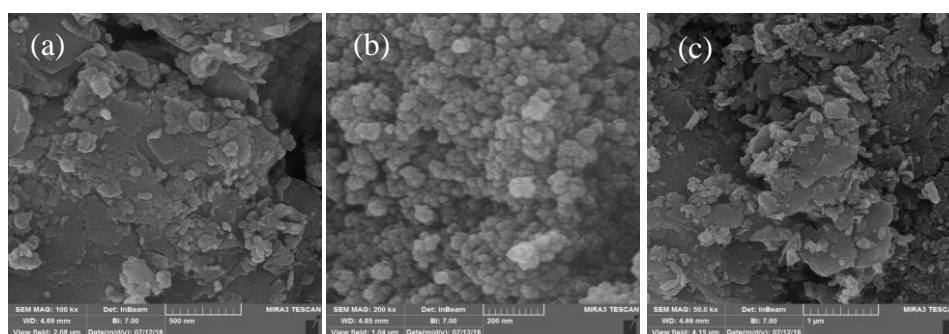


Fig. 4. FESEM analysis of clinoptilolite zeolite (a), Fe<sub>3</sub>O<sub>4</sub> nanoparticles (b), zeolite/Fe<sub>3</sub>O<sub>4</sub> nanocomposite (c)

### The result of VSM analysis

Figure 5 shows the magnetic curve of the samples of  $\text{Fe}_3\text{O}_4$  nanoparticles and zeolite/ $\text{Fe}_3\text{O}_4$  nanocomposite. Both adsorbents are at magnetic ambient temperature and no hysteresis loops are observed in them. Saturation of magnetic  $\text{Fe}_3\text{O}_4$  nanoparticles and zeolite/ $\text{Fe}_3\text{O}_4$  nanocomposite are respectively 49 and 14. As it was expected, the magnetic saturation of zeolite/ $\text{Fe}_3\text{O}_4$  nanocomposite has been lower than  $\text{Fe}_3\text{O}_4$  nanoparticles that are showing the presence of zeolite in nanocomposite causes the decrease of magnetic saturation.

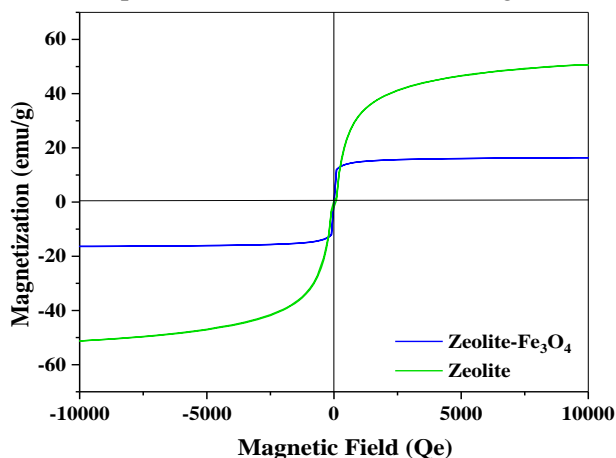


Fig. 5. VSM analysis for zeolite/ $\text{Fe}_3\text{O}_4$  nanocomposite and  $\text{Fe}_3\text{O}_4$  nanoparticles

### The effect of pH on adsorption efficiency of dye

The amount of pH is one of the important parameters in controlling of adsorption process, on the other hand, the adsorbent superficial load and ion load of the dye molecule play an important role in adsorption process [36]. (Figure 6) is presenter of adsorption process of dye that this experiment has been accomplished in pH of 3, 5, 7 and 9. In (Figure 6) was observed that the maximum amount of adsorption of Blue 41 cationic dye has achieved in  $\text{pH}=9$  and the minimum of adsorption has achieved in  $\text{pH}=3$ . Also by attention to (Figure 6-b), the adsorbent level of  $\text{pH} < \text{pH}_{\text{pzc}}$  has positive superficial load in Zeolite/ $\text{Fe}_3\text{O}_4$  nanocomposite and in  $\text{pH} > \text{pH}_{\text{pzc}}$  has negative superficial load [37]. By increasing pH, the amount of adsorption increases due to increasing  $\text{OH}^-$  ion in solution and creation of electrostatic gravity among hydronium ion and cationic dye. As a result, the adsorption decrease of Blue 41 cationic dye in acidic pH ( $\text{pH} < \text{pH}_{\text{pzc}}$ ) can be due to the creation of positive load on zeolite/ $\text{Fe}_3\text{O}_4$  nanocomposite surface, too. The result of study of Farjiet al. were done for removing Blue 41 dye using raw rice husk and modified by using citric acid, the gained result indicates that optimum pH for both adsorbents are about 10 and also the process efficiency has increased by increasing pH [38]. In the survey which has done Jiang et al. in 2013 for the removal of Blue 41 cationic dye using N and stabilized F on  $\text{TiO}_2$ . They concluded that by increasing the pH from 2 to 9, the adsorption capacity has increased from 33.37 mg/g to

93.17 mg/g and the maximum removal efficiency of Blue 41 cationic dye takes place in high pH ( $\text{pH}=8$ ) [39]. Also, in the research which was done by Humelnicu et al. for the removal of Blue cationic dye by ToF natural zeolite, the obtained result of the research showed that the maximum adsorption capacity has been in pH of about 8 [13].

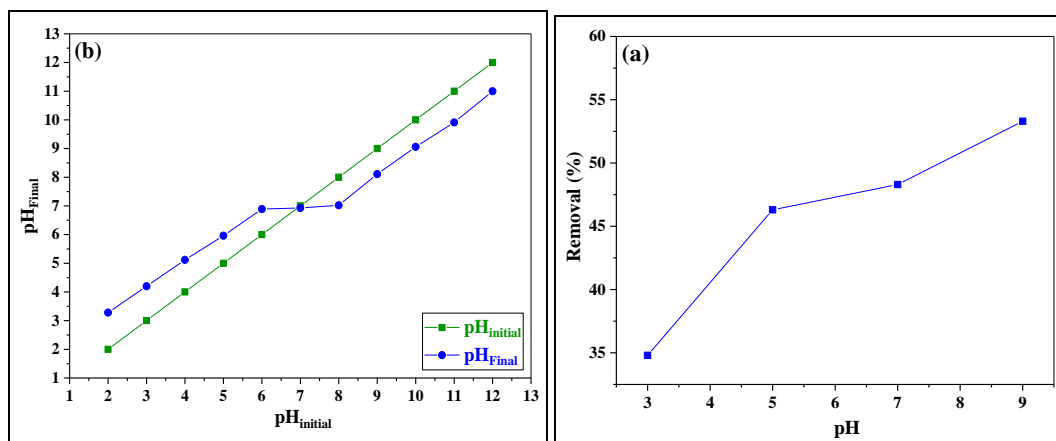


Fig. 6. Surveying the effect of pH in removal process of Blue 41 cationic dye using zeolite/ $\text{Fe}_3\text{O}_4$  nanocomposite (dye concentration of 50 mg/L, adsorbent dose of 1 g/L and contact time of 60 minutes) (a) and investigating  $\text{pH}_{\text{pzc}}$  of nanocomposite (b)



### The effect of adsorbent dose on the adsorption efficiency of dye

Determining the adsorbent dose due to economic surveys is one of the important significant issues in adsorption systems. (Figure 7) shows the adsorption process changes of dye by composite. During the experiments which were done in the samples of 100 mL with concentration of 50 mg/L of dye, contact time of 60 minutes, pH of 9 and with doses of 0.5, 1, 1.5, 2, 3, 4, 5 g/L. It was specified that the rate of removal of Blue 41 cationic dye has increased by increasing the amount of adsorbent. The removal efficiency of Blue 41 dyes by increasing the amount of dose from 0.5 to 3 g/L has increased from 39.7 % to 89.56 % but by increasing the dose up to 5 g/L the rate of removal of dye has achieved to 92.32 % and has almost been steady. Also, the rate of adsorption capacity for dye was calculated based on absorbed dye by each gram of composite. The adsorption capacity has decreased by increasing dose as the adsorption capacity of dye has decreased from 39.7 mg/g to 9.23 mg/g in the doses from 0.5 g/L to 5 g/L; so the optimum dose of experiments was chosen 3 g/L. Increasing the dye adsorption along increasing the dose of adsorbent takes place due to increasing the number of positive sites, increasing the adsorbent level and existence of a strong impelling force [40]. The low number of activate sites are in the hand of dye molecule in low doses of adsorbent that it causes the decrease of removal efficiency. However, the removal efficiency increases by increasing the dose of absorbent, the rate of adsorption capacity decreases due to the saturation some of the existence sites on the adsorbent surface [41]. These results completely agree with Regti et al. findings which they investigated about the removal of dye by using activated carbon [42]. A similar result was obtained in the study which was done about removal of dye with modified adsorbent by Ong et al., too [43].

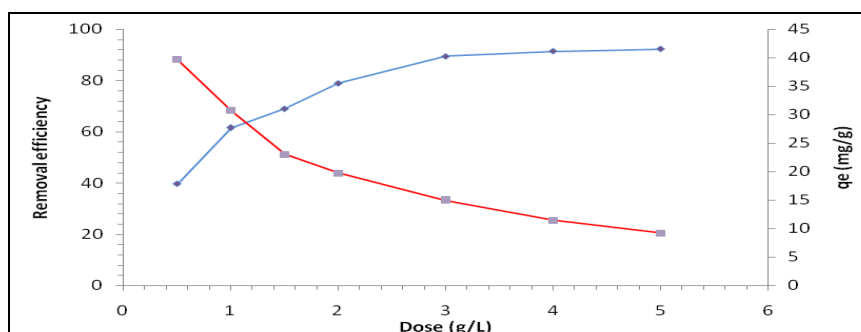


Fig. 7. The effect of dose of zeolite/Fe<sub>3</sub>O<sub>4</sub> nanocomposite on the removal efficiency of Blue 41 cationic dye (initial dye concentration to the amount of removal of dye of 50 mg/L, pH of 9 and contact time of 60 min)

### The effect of contact time on the dye adsorption efficiency

One of the other effective factors in removal of dye is contact time. The adsorption of Blue 41 cationic dye was investigated in the interval of 0 to 160 min. As it is observed in (Fig. 8), mass transmission has taken place in two stages. In the first step adsorption is very fast due to the vacancy of adsorbent activated sites. But by passing the time and gradually filling of adsorbent sites, penetration among the absorbed ions and connection to the empty sites have caused that adsorption operations becoming slower. As a result, the amount of adsorption increases by increasing the contact time and after the quick initial stage has been gradually approaching to the balance and finally approaches to the balance. As it was observed in (Figure 8), close to 91.54 % of total amount of accomplished adsorption occurs in the first 60 min and after wards, adsorption is becoming slower till the adsorption process approaches to the balance within 160 min and residual concentration of dye in the solution didn't change after this time. Because the adsorbent surfaces for certain weight of adsorbent have specific locations for pollutant adsorption has occurred in the pores that adsorption rate decreases in this phase [44]. The obtained results in this research completely agree with the findings of Nasrullah et al. and Parlayıcı et al. [45, 46].

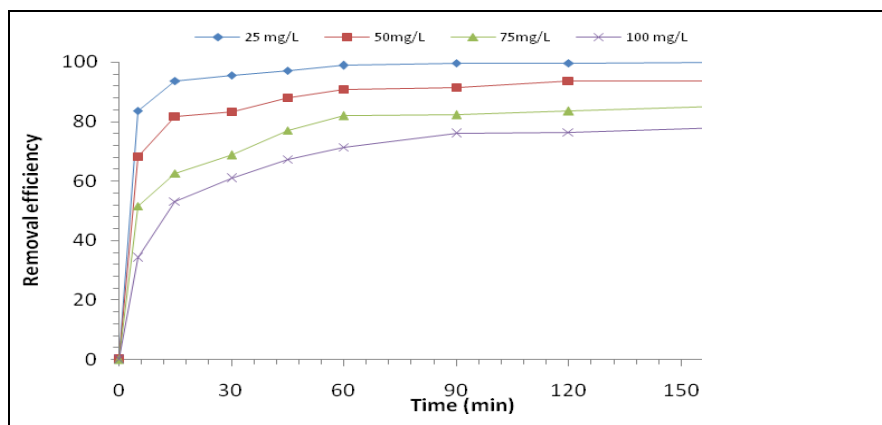


Fig. 8. Surveying the effect of increasing the contact time on the removal efficiency of dye in different concentrations (pH=9, adsorbent dose of 3 g/L and contact time

### The effect of initial dye concentration at equilibrium time on dye adsorption efficiency

Initial concentration of pollutant is the other effective important parameters in adsorption process. Surveying the changes of dye initial concentration determines that by increasing the pollutant concentration, the amount of its adsorption will decrease, too. As it was observed in (Figure 9) the adsorption efficiency decreases by increasing the concentration of Blue 41 dyes from 10 mg/L to 250 mg/L. At low concentration of dye, specific surface and exchanging sites of adsorption have been more and absorbing molecules are capable of having interaction on the adsorbent surface by existing adsorption positions and so adsorption efficiency is more [47]. By increasing initial concentration and being constant of the adsorbent to dyes solution ratio, the rate of adsorption efficiency has decreased due to being saturated the exchanging sites by absorbing substance. This is because of it that there are a lot of exchanging sites at first and they cause increasing in dye adsorption and by decreasing exchanging sites in adsorbent, adsorption efficiency decreases. In the study, which was done by Pavan et al. in 2013, about removal of dye by papaya seed powder was also observed that by increasing amount of pollutant, the efficiency of adsorption decreased that agree with the results of this study [47]. Also the obtained results completely agree with a report that has been presented by Ahmad Reza Bagheri et al. in 2016 about dye removal by the magnetized activated carbon [48]. Also the obtained results completely agree with a report that has been presented by Shirmardi et al. in 2013 about the removal of malachite green dye by carbon nanotubes [49].

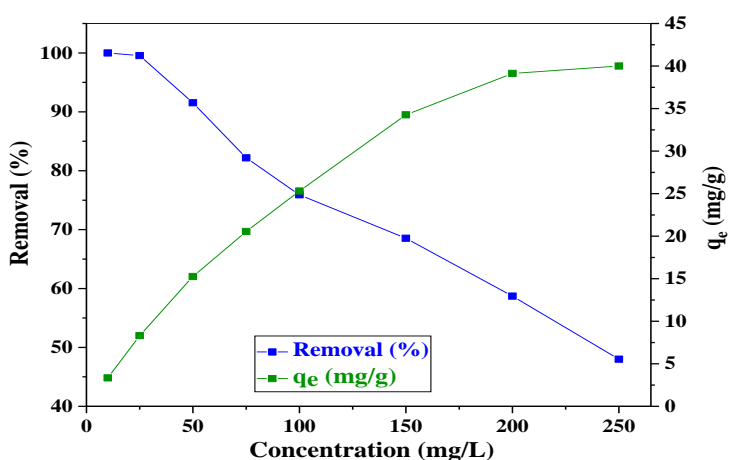


Fig. 9. The effect of concentration changes of Blue 41 cationic dye on the efficiency of Zeolite/Fe<sub>3</sub>O<sub>4</sub> (the amount of adsorbent of 3 g/L, contact time of 90 min)

### Surveying the isotherm process

In order to investigating equilibrium mechanism among pollutant and adsorbent, isotherm was calculated by changing the dye initial concentration. The obtained adsorption data were analyzed by using Langmuir and Freundlich isotherm equations. Langmuir isotherm considers that adsorption is a process which occurs in a specific steady surface. On the other hand, Freundlich isotherm is assumed that a layer of adsorption process takes place on an unsteady surface [50]. The linear equations related to isotherm and kinetics are listed in (table 4) [51, 52]. In equation  $q_e$  is the amount of absorbed substance in mass unit of adsorbent (mg/g),  $C_e$  is equilibrium concentration of absorbing substance in solution after adsorption process (mg/L),  $n$  is adsorption intensity,  $q_m$  is illustrator of adsorption capacity and  $k_l$ ,  $k_f$  are respectively presenter of Langmuir and Freundlich constants. As can be seen from the results of (Figure 10) and (table 5), the adsorption of Blue 41 dyes follows Freundlich isotherm by using of Zeolite/Fe<sub>3</sub>O<sub>4</sub> nanocomposite in present study with the regression coefficient of 0.9839. On the other hand, in this model the amount of  $1/n$  is less than one that is showing this that adsorption of dyes substance on the adsorbent in less concentrations of dye is better than high concentrations of dye and adsorption process is a chemical process [53]. The obtained results completely agreed with presented reports by other studies [54, 55]. (Table 6) shows the comparison of adsorption capacity of different types of adsorbent for Blue 41 cationic dye. The maximum adsorption capacity of Zeolite/Fe<sub>3</sub>O<sub>4</sub> nanocomposite was 36.23 mg/g. Zeolite/Fe<sub>3</sub>O<sub>4</sub> nanocomposite can be considered as a suitable adsorbent due to the high adsorption capacity relative to adsorption of Blue 41 cationic dye, abundance and availability of its precursors and low costs. It can be conducted that the maximum adsorption capacity of Blue 41 cationic dye on Zeolite/Fe<sub>3</sub>O<sub>4</sub> nanocomposite, which has obtained in this study by the other adsorbents that have been tested, is better.



**Table 4**  
LINEAR EQUATIONS OF ISOTHERM AND KINETICS

Kinetic equations		Isothermal equations	
pseudo-first-order	$\log (q_e - q_t) = \log q_e - \left( \frac{k_1 t}{2.303} \right)$	Langmuir	$\frac{1}{q_e} = \frac{1}{k_1 q_m c_e} + \frac{1}{q_m}$
pseudo-second-order	$\frac{t}{q_e} = \frac{1}{(k_2 q_e^2)} + \left( \frac{1}{q_e} \right) t$	Freundlich	$\log q_e = \log k_f + \frac{1}{n} \log c_e$

where  $q_t$  and  $q_e$  are the amount of the dye adsorbed (mg/g) at time  $t$  and at equilibrium time, respectively, and  $k_1$  is the rate constant of adsorption (L/min);  $k_2$  is the equilibrium rate constant calculated for the pseudo-second-order adsorption model (g/mg/min), where  $K_f$  (L/g) is the Freundlich constant and  $n$  shows the intensity level of the adsorption. The plot of  $\ln q_e$  versus  $\ln C_e$  is used to make the intercept  $K_F$  and the slope  $1/n$ . A value of  $1/n$  higher than 1 indicates that saturation is not achieved.  $C_e$  (mg/L) is the initial dye concentration,  $q_e$  (mg/g) is the adsorbate adsorption capacity at the adsorption equilibrium time.  $Q_m$  and  $b$  are the maximum adsorption capacity (mg/g) and the rate constant of Langmuir (L/mg), respectively. The  $R_L$  values between 0 and 1 indicate favorable adsorption.

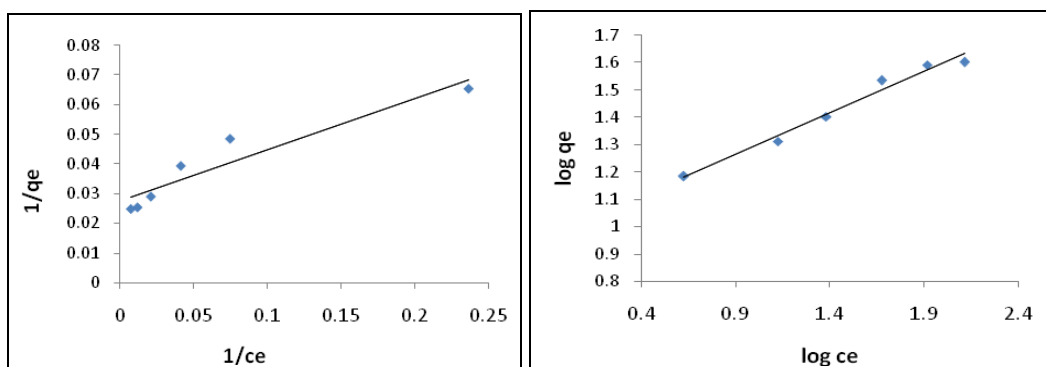


Fig. 10. Langmuir (a) and Freundlich (b) isotherm model in dye adsorption on Zeolite/Fe<sub>3</sub>O<sub>4</sub> nanocomposite

**Table 5**  
PARAMETERS OF LANGMUIR AND FREUNDLICH MODEL  
IN DIFFERENT CONCENTRATION

Langmuir isotherm				Freundlich isotherm		
$q_m$ (mg/g)	$K_L$ (L/mg)	$R^2$	$R_L$	$K_f$ (L/g)	$n$	$R^2$
36.23	0.195	0.8945	0.111	9.75	3.28	<b>0.9839</b>

**Table 6**  
THE COMPARISON OF MAXIMUM ADSORPTION CAPACITY ( $Q_{MAX}$ )  
OF DIFFERENT ADSORBENTS FOR BLUE 41 CATIONIC DYE

Adsorbent type	pH	$q_{max}$ (mg/g)	Reference
Sodium alginate	8	12	[56]
Raw rice husk	10	24	[38]
Modified rice husk	10	35	[38]
Zinc oxide Nano powder into hybrid beads	7	16.5	[54]
Fe <sub>3</sub> O <sub>4</sub> /Zeolite	9	36.23	Present study

### Surveying the kinetics process

The kinetic equations are investigated to describe the behavior of transferring of absorbing substance molecules and effective factors on adsorption process rate. In this study, the adsorption kinetics of pseudo first order and pseudo second order were surveyed in different concentrations under optimum conditions in different moments for adsorption process of Blue 41 cationic dye. The kinetic equations of pseudo first order are illustrative of it that penetration takes place in a layer and is biased on adsorption capacity in which the changes in the amount of adsorption with time, is proportional to the number of unoccupied sites in adsorbent surface [57]. The kinetics of pseudo second order indicates that the chemical adsorption of stage slows down the rate and controls adsorption processes [58]. The

kinetics equations of pseudo first and second order are presented linearly in (table 4). In this equation,  $q_e$  and  $q_t$  are adsorption capacity in equilibrium phase and  $t$  time respectively and also,  $k_1$  and  $k_2$  are the rate coefficient of pseudo first order and pseudo second order. By attending to the constant coefficients and the obtained correlation in (table 7) and by attending to (Figure 11) can present that the desired process follows the pseudo second order kinetic model and the chemical adsorption of stage has been the limiter in adsorption process. Also, the most part of adsorption is carried out in form of chemical adsorption that the obtained results of process of isotherm confirm this claim, too [59]. On the other hand, the results indicate (table 7) that by increasing the dye concentration from 25 mg/L to 100 mg/L, the constant amount of reaction rate decreases from 0.123 to 0.005 which this phenomenon shows that the rate of adsorption process decreases by increasing the pollutant concentration. Liangguo Yan et al., in their study, which has done on the removal of heavy metals using magnetized bentonite, achieved similar results [33]. Also, in the study that Naddafi and Gholami carried out to remove surfactant dye, the obtained results showed that kinetics of adsorption of this dye has followed pseudo second order model [3].

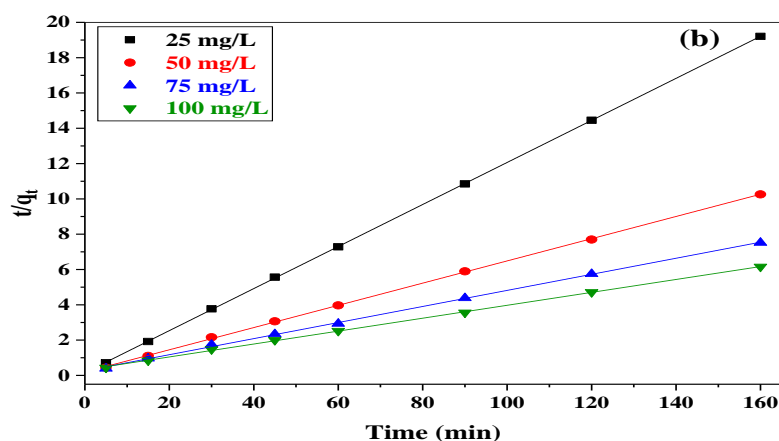


Fig. 11. Pseudo first order (a) and pseudo second order (b) kinetic model in dye adsorption on Zeolite/Fe<sub>3</sub>O<sub>4</sub> nanocomposite

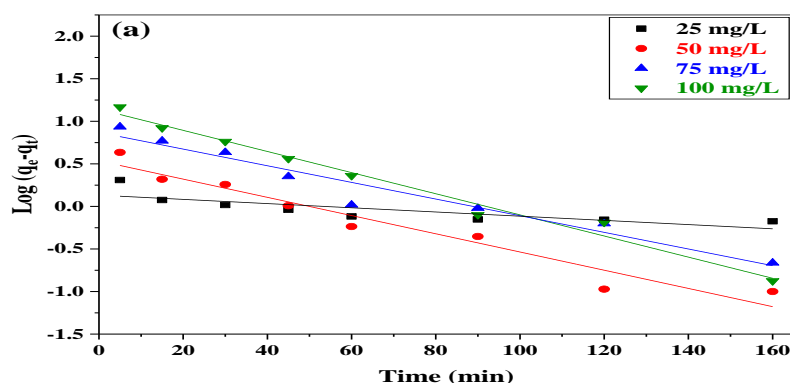


Table 7  
KINETIC PARAMETERS OF DYE ADSORPTION IN OPTIMUM CONDITIONS  
AND DIFFERENT CONCENTRATIONS

Dye concentration (mg/L)	$q_e$ , exp.	Pseudo first order			Pseudo second order		
		$q_{e1}$ , cal.	$k_1$	$R^2$	$q_{e2}$ , cal.	$k_2$	$R^2$
25	9	1.35	0.005	0.6606	8.36	0.123	0.9999
50	15.7	3.42	0.024	0.9458	15.77	0.027	0.9995
75	21.5	7.40	0.022	0.9483	21.64	0.010	0.9984
100	26.1	13.87	0.028	0.9837	26.80	0.005	0.9974

#### Adsorbent recovery

In an economic point of view, recovery of adsorbents is important; the chemical method has the most application in recovery of adsorbents. In chemical recovery, molecules of dye substitute by adsorbent surface in dissolved solution or through ion exchange. Recovery of Zeolite/Fe<sub>3</sub>O<sub>4</sub> nanocomposite carried out by using of NaOH of 0.1 M. Generally, can be seen that the adsorption capacity of nanocomposite decreases by increasing the number of recovery cycle. Figure 12 shows that recovery of Zeolite/Fe<sub>3</sub>O<sub>4</sub> nanocomposite by NaOH of 0.1 M, the efficiency of Blue 41 cationic dye approached from 89.56 % to 40.79 % after the fifth stage. The high concentration of NaOH ions compete

with Blue 41 cationic dye which position in activated sites and Blue 41 cationic dye separates from activated sites and adsorbent becomes recovery. Therefore can be concluded that Zeolite/Fe<sub>3</sub>O<sub>4</sub> nanocomposite has high potential for waste water treatment of dyes industries, because it can be reused by adsorbent recovery and by its ability in maintaining the removal efficiency after five consecutive period so cost efficiency will be economical and are very important for industrial applications, too until be avoided from secondary pollutions in sewage treatment [60].

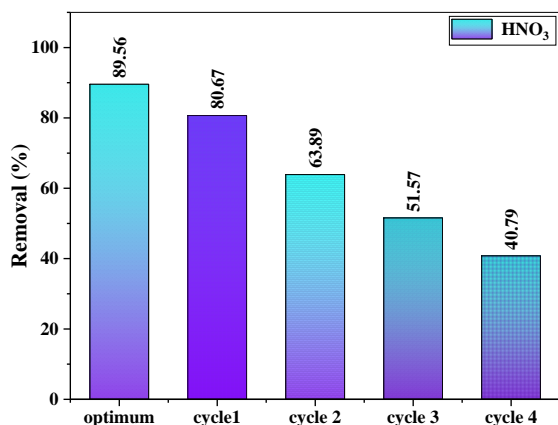


Fig. 12. Zeolite/Fe<sub>3</sub>O<sub>4</sub> nanocomposite recovery stages

## Conclusions

This research has shown significant effectiveness Zeolite/Fe<sub>3</sub>O<sub>4</sub> nanocomposite in adsorption of Blue 41 cationic dye from aqueous solutions in a wide range of concentrations. Analyzes of FTIR, XRD, FESEM, VSM and XRD have confirmed the nature and the structure of Zeolite/Fe<sub>3</sub>O<sub>4</sub> nanocomposite adsorbent. The obtained results and analyzes determined that adsorption process efficiency increases by increasing reaction time, pH and amount of adsorbent and versus, increasing dye initial concentration causes significant decrease of adsorption efficiency. The obtained results of adsorption of isotherm and kinetics study illustrated that data follows Freundlich model and pseudo second order kinetics. Under optimum conditions of pH=9, dye initial concentration of 100 mg/L, adsorbent dose of 3 g/L and reaction time of 60 min, removal efficiency was obtained 71.4%. Totally results showed that Zeolite/Fe<sub>3</sub>O<sub>4</sub> nanocomposite can be used by scrutiny of operating conditions of the adsorption process as a adsorbent with high effectiveness and availability, eco-friendly and cost-effective in order to removing dye from waste water of different industrials. Zeolite is readily available as a cheap material in various countries. Zeolite and its compounds can be a good alternative to other expensive adsorbents.

*Acknowledgment: The authors would like to acknowledge Ardabil University of Medical Sciences (code: IR.ARUMS.REC) for financial and instrumental supports.*

## References

1. CHATTERJEE, S., CHATTERJEE, T., WOO, S.H., Chemical Engin.J., **166**, 2011, p. 168
2. GONG, J.L., WANG, B., ZENG, G.M., YANG, C.P., NIU, C.G., NIU, Q.Y., J.Hazard.Mater., **164**, 2009, p. 1517
3. NADDAFI, K., GHOLAMI, M., Iran.J.Health and Environ., **7**, 2014, p. 277
4. OTHMANI, A., KESRAOUI, A., SEFFEN, M., Euro-Mediterran.J.Environ.Integrat., **2**, 2017, p. 6
5. DOS SANTOS, A.B., CERVANTES, F.J., VAN LIER, J.B., Bioresource Technol., **98**, 2007, p. 2369
6. RAHMANI, A.R., ASGARI, G., FARROKHI, M., Iran.J.Health and Environ., **5**, 2013, p. 509
7. SALAHSHOOR, Z., SHAHBAZI, A., BADIEI, A., Water and Waste Water, **27**, 2016, p. 19
8. ATAR, N., OLGUN, A., ÇOLAK, F., Engin.Life Scien., **8**, 2008, p. 499
9. ABBASI, M., ASL, N.R., J.Hazard.Mater., **153**, 2008, p. 942
10. BOUAFIA-CHERGHI, S., OTURAN, N., KHALAF, H., OTURAN, M.A., J.Environ.Scienc.Health-Part A., **45**, 2010, p. 622
11. JIANG, Y., SUN, Y., LIU, H., ZHU, F., YIN, H., Dyes and Pigments, **78**, 2008, p. 77
12. NOROOZI, B., SORIAL, G., BAHRAMI, H., ARAMI, M., J.Hazard.Mater., **139**, 2007, p. 167
13. HUMELNICU, I., BĂICEANU, A., IGNAT, M.E., DULMAN, V., Process Safety and Environ.Protec., **105**, 2017, p. 274
14. GUPTA, V., CARROTT, P., RIBEIRO CARROTT, M., Critical Rev.Environ.Scienc. Technol., **39**, 2009, p. 783
15. MALAKOOTIAN, M., ASADIPOUR, A., MOHAMMADI, S., J.Sabzevar Univ. Medical Scien., **23**, 2016, p. 110
16. OMRI, A., BENZINA, M., TRABELSI, W., AMMAR, N., Desalin.Water Treat., **52**, 2014, p. 2241
17. MALEKI, A., MAHVI, A.H., REZAEI, R., DAVARI, B., Iran.J.Health and Environ., **5**, 2013, p. 519
18. HAGHIGHI, M., RAHMANI, F., DEGHANI, R., TEHRANI, A.M., MIRANZADEH, M.B., Desalin.Water Treat., **58**, 2017, p. 168
19. NOURISEPEHR, G., EMTIAZJOO, M., NOURISEPEHR, M., DEGHANIFARD, E., J.Environ.Health Engin., **3**, 2016, p. 337
20. JONIDI JAFARI, A., REZAEI KALANTARY, R., BABAEI, A.A., HEYDARI FARSANI, M., KAKAVANDI, B., J.Mazandaran Univ.Medical Scien., **26**, 2016, p. 171
21. AFSHIN, S., MOKHTARI, S.A., VOSOUGHI, M., SADEGHI, H., RASHTBARI, Y., Data in brief., **21**, 2018, p. 1008
22. NIRI, M.V., MAHVI, A.H., ALIMOHAMMADI, M., SHIRMARDI, M., GOLASTANIFAR, H., MOHAMMADI, M.J., J.Water and Health., **13**, 2015, p. 394
23. YUANBI, Z., ZUMIN, Q., HUANG, J., Chinese J.Chem.Engin., **16**, 2008, p. 451

24. FAZLZADEH, M., KHOSRAVI, R., ZAREI, A., *Ecological Engin.*, **103**, 2017, p. 180
25. TORRES-PÉREZ, J., GÉRENTE, C., ANDRÈS, Y., *Chinese J.Chem.Engin.*, **20**, 2012, p. 524
26. RASHTBARI, Y., HAZRATI, S., AFSHIN, S., FAZLZADEH, M., VOSOUGHI, M., *Data in brief.*, **20**, 2018, p. 1434
27. NADAFI, K., VOSOUGHI, M., ASADI, A., BORNA, M.O., SHIRMARDI, M., *J.Water Chem.Technol.*, **36**, 2014, p. 125
28. MOHSENI-BANDPI, A., AL-MUSAWI, T.J., GHAHRAMANI, E., ZARRABI, M., MOHEBI, S., VAHED, S.A., *J.Molec.Liq.*, **218**, 2016, p. 615
29. KUŹNIARSKA-BIERNACKA, I., FONSECA, A.M., NEVES, I.C., *Inorg.Chim.Acta*, **394**, 2013, p. 591
30. GONG, R., ZHU, S., ZHANG, D., CHEN, J., NI, S., GUAN, R., *Desalination*, **230**, 2008, p. 220
31. TORABIAN, A., KAZEMIAN, H., SEIFI, L., BIDHENDI, G.N., AZIMI, A.A., GHADIRI, S.K., *Clean-Soil, Air, Water*, **38**, 2010, p. 77
32. HASHEMIAN, S., *Main Group Chem.*, **6**, 2007, p. 97
33. YAN, L., LI, S., YU, H., SHAN, R., DU, B., LIU, T., *Powder Technol.*, **301**, 2016, p. 632
34. IKHTIYAROVA, G., ÖZCAN, A., GÖK, Ö., ÖZCAN, A., *Clay Minerals*, **47**, 2012, p. 31
35. DUMAN, O., TUNÇ, S., POLAT, T.G., BOZOĞLAN, B.K., *Carbohydrate polym.*, **147**, 2016, p. 79
36. TAKDASTAN, A., MAHVI, A.H., LIMA, E.C., SHIRMARDI, M., BABAEI, A.A., GOUDARZI, G., *Water Scien.Technol.*, **74**, 2016, p. 2349
37. ÇALIŞKAN, E., GÖKTÜRK, S., *Separation Scien.Technol.*, **45**, 2010, p. 244
38. KARAJ, I., *J.Occupat.Enviroin.Health.*, **1**, 2016, p. 41
39. JIANG, Y., LUO, Y., ZHANG, F., GUO, L., NI, L., *Appl.Surf.Sci.*, **273**, 2013, p. 448
40. KHOSRAVI, R., ZAREI, A., HEIDARI, M., AHMADFAZELI, A., VOSUGHI, M., FAZLZADEH, M., *Korean J.Chem.Engin.*, **35**, 2018, p. 1000
41. ABDOALLAHZADEH, H., ALIZADEH, B., KHOSRAVI, R., FAZLZADEH, M., *J.Mazandaran Univ.Medical Scien.*, **26**, 2016, p. 111
42. REGTI, A., LAAMARI, M.R., STIRIBA, S.E., EL HADDAD, M., *Microchem.J.*, **130**, 2017, p. 129
43. ONG, S., LEE, C., ZAINAL, Z., *Bioresource Technol.*, **98**, 2007, p. 2792
44. AUTA, M., HAMEED, B., *Environ.Engin.Manag.J.*, **14**, 2015, p. 955
45. NASRULLAH, A., BHAT, A., NAEEM, A., ISA, M.H., DANISH, M., *Int.J.Biol. Macromol.*, **107**, 2018, p. 1792
46. PARLAYICI, Ş., PEHLIVAN, E., *Powder Technol.*, **317**, 2017, p. 23
47. PAVAN, F.A., CAMACHO, E.S., LIMA, E.C., DOTTO, G.L., BRANCO, V.T., DIAS, S.L., *J.Environ.Chem.Engin.*, **2**, 2014, p. 230
48. BAGHERI, A.R., GHAEDI, M., ASFARAM, A., BAZRAFSHAN, A.A., *Ultrason.Sonochem.*, **34**, 2017, p. 294
49. SHIRMARDI, M., MAHVI, A.H., HASHEMZADEH, B., NAEIMABADI, A., HASSANI, G., *Korean J.Chem.Engin.*, **30**, 2013, p. 1603
50. TAN, I., AHMAD, A., HAMEED, B., *J.Hazard.Mater.*, **154**, 2008, p. 337
51. ZHANG, L., HU, P., WANG, J., HUANG, R., *Appl.Surf.Sci.*, **369**, 2016, p. 558
52. MASSOUDINEJAD, M., ASADI, A., VOSOUGHI, M., GHOLAMI, M., KARAMI, M.A., *Korean J.Chem.Engin.*, **32**, 2015, p. 2078
53. KHALED, A., EL NEMR, A., EL-SIKAILY, A., ABDELWAHAB, O., *J.Hazard.Mater.*, **165**, 2009, p. 100
54. HASSAN, H.S., ELKADY, M., EL-SHAZLY, A., BAMUFLEH, H.S., *J.Nanomater.*, **2014**, 2014, p. 6
55. ALVER, E., METIN, A.Ü., *Chem.Engin.J.*, **200**, 2012, p. 59
56. MAHMOODI, N.M., HAYATI, B., ARAMI, M., *Ind.Crops Prod.*, **35**, 2012, p. 295
57. MOMENZADEH, H., TEHRANI-BAGHA, A.R., KHOSRAVI, A., GHARANJIG, K., HOLMBERG, K., *Desalination*, **271**, 2011, p. 225
58. GHAEDI, M., GHAEDI, A., HOSSAINPOUR, M., ANSARI, A., HABIBI, M., ASGHARI, A., *J.Ind.Engin.Chem.*, **20**, 2014, p. 1641
59. KAKAVANDI, B., JONIDI, A., REZAEI, R., NASSERI, S., AMERI, A., *Iran.J.Environ. Health Scien.Engin.*, **10**, 2013, p. 19
60. CHIENG, H.I., LIM, L.B., PRIYANTHA, N., *Environ.Technol.*, **36**, 2015, p. 86

Manuscript received: 27.06.2017